

Histopathological Image Classification and Vulnerability Analysis using Federated Learning

Sankalp Vyas

*Computing and Information Science
Anglia Ruskin University, Cambridge
sankalp.vyas@student.aru.ac.uk*

Amar Nath Patra

*Radford University
Radford, USA
apatra@radford.edu*

Raj Mani Shukla

*Computing and Information Science
Anglia Ruskin University, Cambridge
raj.shukla@aru.ac.uk*

Abstract—Healthcare is one of the foremost applications of machine learning (ML). Traditionally, ML models are trained by central servers, which aggregate data from various distributed devices to forecast the results for newly generated data. This is a major concern as models can access sensitive user information, which raises privacy concerns. A federated learning (FL) approach can help address this issue: A global model sends its copy to all clients who train these copies, and the clients send the updates (weights) back to it. Over time, the global model improves and becomes more accurate. Data privacy is protected during training, as it is conducted locally on the clients' devices.

However, the global model is susceptible to data poisoning. We develop a privacy-preserving FL technique for a skin cancer dataset and show that the model is prone to data poisoning attacks. Ten clients train the model, but one of them intentionally introduces flipped labels as an attack. This reduces the accuracy of the global model. As the percentage of label flipping increases, there is a noticeable decrease in accuracy. We use a stochastic gradient descent optimization algorithm to find the most optimal accuracy for the model. Although FL can protect user privacy for healthcare diagnostics, it is also vulnerable to data poisoning, which must be addressed.

Index Terms—Healthcare, Federated learning, Deep neural network, Label flipping, Data poisoning

I. INTRODUCTION

In machine learning (ML), models are trained that use patterns in data to make predictions and decisions. A large amount of data is collected from multiple sources and aggregated in one location for training and evaluation. ML has potential in healthcare: By training models on medical data, tailored treatment regimens can be developed, epidemic diseases can be predicted, and trends or patterns in medical data can be identified, leading to new medicines or cures [1], [2]. However, collecting and merging data can put the privacy of individuals and organizations at risk, as they may contain confidential or personal details. Additionally, transmitting massive data via the Internet can be slow and costly.

Federated learning (FL) [3] overcomes these challenges by training local models on devices without data exchange. Instead of actual data, the global model is sent to these decentralized data sources and trained remotely. Additionally, FL enables model training using data controlled by numerous organizations, each of which may have different privacy concerns. Therefore, organizations can still benefit from the benefits of integrated data while protecting their privacy.

The importance of FL is especially pronounced when it comes to sensitive data, such as healthcare records, that are available from multiple sources. For example, automated classification of skin lesions assists dermatologists in making faster and more accurate decisions based on ML [4]. Although ML-based systems show a decent performance in automatically classifying skin-lesion images, they need a huge amount of data that needs to be gathered for training such models. Such data is available in different hospitals and at different locations. Therefore, one of the problems encountered while developing such an automated tool is that the skin-lesion data are available across different hospitals. These data may not be shared between them due to privacy concerns and regulations.

To solve this issue, we develop a privacy-preserving Machine Learning method for the automated classification of skin lesions that employs federated learning. The advantage of the proposed approach is that the raw patient data need not be shared with the AI service developer, and hence patient privacy is preserved. The proposed approach makes it easy to develop an AI model using a large dataset that is spatially located. Although the proposed approach is beneficial, there is a security risk of malicious or dishonest hospitals, as they could introduce vulnerabilities into the system by sending incorrect updates. One of the strategies that they can carry out is training their local model after flipping the labels to diminish the effectiveness of the global model. Therefore, we also investigate the vulnerabilities of the proposed approach for skin lesion classification that needs to be tackled for the practical realization of such a distributed learning system.

The rest of the paper is organized as follows. Section 2 describes previous research based on FL and label-flipping attacks. The details of the preprocessing, preparation of the dataset, and the setup for building the FL model will be presented in Section 3. Furthermore, this section provides a description of the technologies used in this research. Section 4 discusses the implementation of the FL model and demonstrates the label-flipping attack. Section 5 compares the outcomes with the earlier studies in this similar area. In Section 6 the future work for this research is discussed and Section 7 concludes the work.

II. LITERATURE REVIEW

This section examines the motivations and challenges of privacy-preserving ML, the current state of privacy-preserving machine learning, focusing on FL and distributed machine learning, and state-of-the-art skin lesion classification algorithms.

A. Motivations and Challenges for Privacy Protection in ML

There are many reasons why privacy is important in ML, but ethical concerns are a significant factor. The use of personal data in ML models raises concerns about possible misuse of sensitive information, including financial or medical records [5]. This can result in adverse outcomes for individuals, such as discrimination and loss of autonomy [6]. Maintaining privacy in ML is crucial due to legal obligations. The European Union (EU), for instance, enforces strict regulations, including the General Data Protection Regulation (GDPR), which restrict the usage of personal data [7]. The purpose of these regulations is to safeguard the privacy of individuals and grant them authority over their personal information. Non-compliance with these guidelines may lead to significant penalties and damage to a business's reputation. Despite these motivations, protecting privacy in ML presents numerous obstacles. One difficulty is the compromise between privacy and utility. Effective ML models require enormous volumes of data, yet the collection and use of these data can compromise individuals' privacy [8]. Maintaining privacy while meeting the demand for data can be a difficult task to balance. Another challenge is to ensure privacy protection against attacks, including membership-inference attacks. These attacks aim to determine whether a person's data was used in training a model [9]. The complexity of privacy-preserving procedures is another obstacle. It can be difficult to modify ML algorithms that operate on raw data without compromising their efficiency and privacy protection [10]. Implementing new techniques can be a time-consuming and resource-intensive process.

B. Privacy-Preserving ML

Privacy-preserving ML pertains to the creation of algorithms and protocols that allow the analysis of data while upholding individuals' privacy. The use of privacy-enhancing technologies (PETs) that protect privacy through technical means, such as encryption and anonymization, is one way to achieve privacy protection in ML [11]. On the other hand, differential privacy achieves privacy preservation by adding noise to the data to obscure the contribution of individual data points [12]. Another technique uses secure multiparty computation (SMC), which allows for the computation of functions over distributed data without the need to share the raw data [13]. FL is a decentralized ML method that enables model training using distributed data without the need to centralize or share raw data [3].

C. Skin Lesion Image Classification

ML has been used to detect and classify skin lesions in a number of studies. Gessert et al. propose a deep learning

model, consisting of a convolution neural network (CNN) and a dense neural network, for classification based on dermoscopic images and additional patient metadata [14]. The classification method designed by Yao et al. [15] consists of modified deep convolution neural networks (DCNN) and a novel Multi-weighted New Loss function that counters class imbalance, improves the accuracy of key classes, and reduces outlier interference. Zhang et al. propose an attention residual learning convolutional neural network (ARL-CNN) model that combines residual learning and a novel attention learning mechanism to improve the discriminative representation ability of DCNNs [16]. Wang et al. present a lightweight two-stage framework, called G-DMN [17], that uses CycleGAN for data augmentation and Dense-MobileNetV2 (DMN) for classification. Mahbod et al. develop a fully automatic computerized classification method [18] that fuses deep features from several robust CNNs, including AlexNet, VGG16, and ResNet-18, and different abstraction levels.

The aforementioned research employs a centralized approach in which skin lesions are collected from different locations, compromising user privacy. In contrast, we propose a FL-based approach to preserve user privacy that does not collect raw data in one place. Instead, the intelligence in the form of trained models is shared between and combined to develop the ML model. Additionally, we analyze the vulnerability of such a system due to the presence of possible malicious clients.

III. METHODOLOGY

This section describes the proposed FL-based approach along with the system model and the data poisoning vulnerability scenario.

A. System model

Fig. 1 presents the system model of the proposed distributed learning environment for histopathological image classification. A hospital $h[i]$ holds raw private images of its patients, which it processes for clean images. Based on the clean dataset, $h[i]$ can train its local model A_i . The application developer, who may represent a company providing Software as a Service (SaaS), is at the other end and does not have access to the raw data. However, the local models from different hospitals are shared through a secure channel with the application developer aggregator. The developer combines these models to create a global model AI that is deployed in the cloud or on the edge as a SaaS platform. This platform can be used by any hospital or individual, regardless of whether they participate in model training. The business model may allow entities participating in the training process to use the platform for free or at a discounted price, while entities not participating in the training process must pay full subscription rates. With more entities participating in the training process and sharing intelligence through their respective trained models, a better global model is developed.

As new data are continuously collected, participants in the training process can retrain the model, using the global

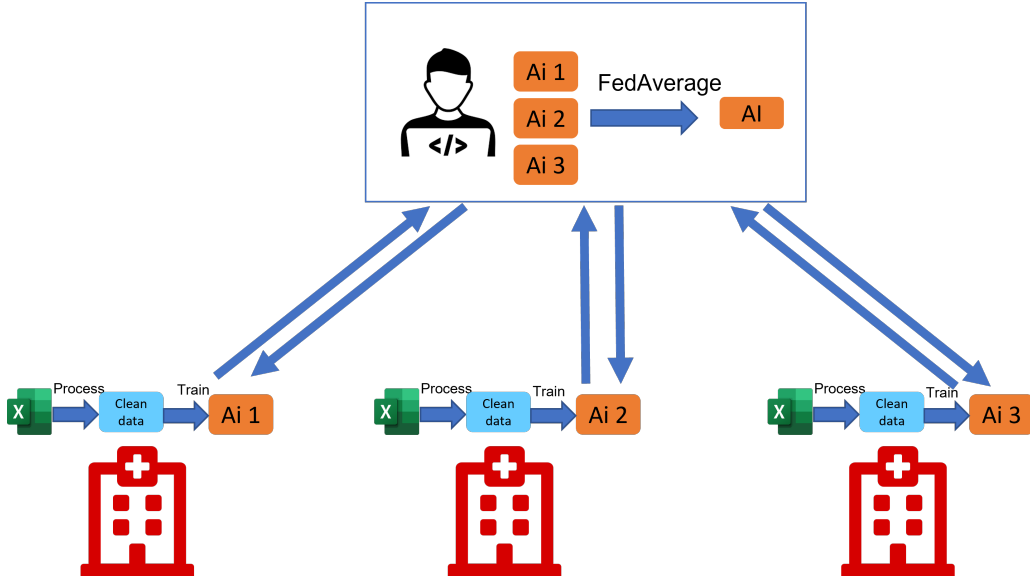


Fig. 1: The distributed learning environment for the proposed Histopathological image classification

model’s weights as initial weights. Over time, the SaaS platform can improve itself as it captures disparate and varied distributions of data.

B. Proposed FL-based approach

As the proposed methodology uses FL, the training dataset D is not fully available on a centralized server but on multiple participants $h[i]$, who have their own private dataset D_i . Each $h[i]$ executes stochastic gradient descent (SGD) locally on its own data and then sends its updated model parameters $\theta_{r,i}$ to the aggregator. The aggregator combines the parameters received to create global parameters θ_r , which are broadcast to all participants $h[i]$. This process is repeated for a fixed number of rounds R and the final model AI_M is created using the global parameters of the last round θ_R .

The deep neural network (DNN) model takes the features f_i and outputs the predicted probabilities p_i for each skin lesion class label c_i in a set of all possible class values C . The predicted class for a given instance x_i is determined by finding the class label with the highest predicted probability. The goal of training the DNN is to find the model parameters θ that minimize the chosen loss function L using iterative SGD. In SGD, a batch of samples B is selected from the dataset D , and the corresponding gradient g_B is computed. The model parameters θ are then updated in the direction of the negative gradient. This process is repeated for multiple epochs.

In the process of training a DNN, dataset D with a set of features f_i and class labels c_i is used, along with a loss function L . This loss function is given by

$$L_{total} = \frac{1}{n} \sum_i^n L(\theta, x_i) \quad (1)$$

The proposed method uses the Federated Averaging (FedAvg) model, a distributed machine learning algorithm de-

signed for model training in a federated setting, where multiple clients or devices, each with their own training data and computational resources, train a shared model. FedAvg’s goal is to train a model capable of making accurate predictions on the data of all clients, even though the data of each client are only a subset of the total data [19]. The hospitals act as the clients in the proposed method.

The overview of the FedAvg algorithm for the proposed histopathological image classification is described below.

- **Initialization** The algorithm begins by initializing the global model AI with random weights and biases. AI is then distributed to each hospital $h[i]$ which uses it as its local model A_i .
- **Communication rounds** The algorithm goes through a series of communication rounds (federated learning rounds) with the following steps in each round
 - **Local training** Each $h[i]$ chooses a subset of its data D_i (mini-batch) to train with. Then, using the selected data, it performs one or more gradient descent steps on its local model A_i .
 - **Averaging** Each $h[i]$ updates the model parameters $\theta_{r,i}$ and sends them to the aggregator. The received models are then averaged together by the aggregator to create a new global model AI .
 - **Update AI** is then returned to the $h[i]$ s to use as local models A_i s.
 - **Repeat** The process repeats until AI reaches a certain level of accuracy of a stopping criterion.

The averaging step in the FedAvg algorithm is crucial, as it updates AI by taking the average of the A_i s. This allows the algorithm to account for differences in data across $h[i]$ s, which can help improve AI ’s generalization performance.

C. Malicious clients

Although the aforementioned approach preserves user privacy, there exists a vulnerability if one or more $h[i]$ s provide incorrect model updates. A hospital $h[i]$ may adopt the following steps to alter the outcome of the global model AI

- 1) Select k samples from the labeled dataset where k is the p percentage of the selected labels
- 2) For each k replace the skin-lesion class with an alternate random skin-lesion class
- 3) Repeat step 2 for all k
- 4) Train the local model A_i on the substituted label
- 5) Send the trained model to the aggregator for Fedaveraging.

IV. PERFORMANCE EVALUATION AND RESULTS

In this section, we provide the details of implementation that include the FL environment setup, DNN architecture, data collection, analysis, visualization, dataset pre-processing, and evaluation methods employed to obtain the results. We analyze the results before and after the flipping of the labels and do a comparative study.

A. Implementation details

1) *FL setup*: The FL system is implemented in the TensorFlow library [20], available in Python. N represents the number of participating hospitals in the FL setup which is set to 10, whereas there is one aggregator. Additionally, independent and identity-distributed data (IID) are used.

2) *Deep neural network architecture*: In the setup, we use a multilayer-perceptron model (MLP) to classify images from the dataset into one of the seven classes. The MLP model consists of three fully connected (dense) layers with 200 units in each. Relu activation is used in the hidden layer and softmax in the output layer.

Each hospital $h[i]$ is responsible for training its local model A_i on its local dataset D_i . We use the SGD optimizer to train the AI model. We train the model for 100 communication rounds, during which the updates from each $h[i]$ are aggregated on the central server and used to update the global model AI . To measure the error of the model during training, we use the categorical_crossentropy loss function. To evaluate the performance of the model, we use the *accuracy* metric, which measures the proportion of correct predictions made by the model.

3) *Data collection*: We use the HAM10000 dataset that consists of a total of 10,015 samples that belong to seven different classes [21]. Fig. 2 shows the image data for all 10,015 samples and the seven classes.

4) *Data analysis and visualization*: The seven classes of skin cancer lesions in the HAM10000 dataset are Melanocytic nevi (nv), Melanoma (mel), Benign keratosis-like lesions (bkl), Basal cell carcinoma (bcc), Actinic keratoses (akiec), Vascular lesions (vasc), and Dermatofibroma (df). Fig. 3 shows some of the samples of the seven different types of lesions.

	pixel0000	pixel0001	pixel0002	pixel0003	pixel0004	pixel0005	pixel0006	pixel0007	pixel0008	pixel0009	...	pixel0775	pixel0776	pixel0777	pixel0778
0	169	171	170	177	181	182	181	185	194	192	...	184	186	185	180
1	19	57	105	140	149	148	144	155	170	170	...	172	175	160	144
2	155	163	161	167	167	172	155	152	165	175	...	163	178	157	166
3	25	71	116	139	136	153	148	161	172	162	...	125	135	138	137
4	129	162	181	196	205	208	205	213	225	224	...	210	197	172	190
...
10010	172	171	173	175	164	187	207	210	208	206	...	210	217	221	209
10011	2	34	108	116	114	119	131	139	139	145	...	173	169	168	168
10012	122	154	162	170	179	197	200	195	202	199	...	221	215	205	187
10013	137	143	141	139	147	152	155	152	155	159	...	172	171	175	183
10014	149	157	157	152	151	152	154	163	149	145	...	159	154	145	106

10015 rows × 785 columns

Fig. 2: Sample skin lesion data

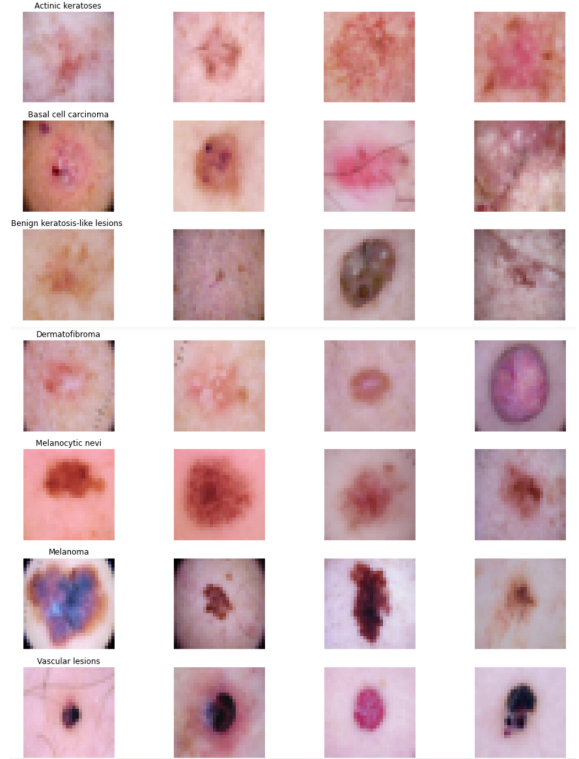


Fig. 3: Types of skin lesions and their samples

5) *Pre-processing of the dataset*: In the pre-processing stage, each pixel in the image is represented by a single greyscale value (ranging from 0 to 255). When these images are stored in a numerical array, they will have 784 elements (28x28), each representing the greyscale value of a single pixel. Thus, there are a total of 784 columns and 10,015 rows. Table I shows the image columns containing values between 0 and 1. The images have been converted to a 1D array as we use MLP to build our FL model. Pixel000, pixel001..., pixel0784, etc. represent the number of pixels while 0,1,2,3,4..., 10,014 indicate the total number of samples.

6) *Evaluation methods*: The metrics used for evaluation are precision, recall, f1-scores, and accuracy (Table II). Precision is the number of true positive predictions divided by the number of true positive plus false positive predictions. The number of true positive predictions divided by the number of true positive plus false negative predictions is recall. Accuracy is the percentage of correct predictions made by the model out of all the predictions made by the model, while the F1 score

TABLE I: Image data after getting scaled between 0 and 1

pixel0000	pixel0001	pixel0002	pixel0003	pixel0004	pixel0005	pixel0006	pixel0007	pixel0008	pixel0009
0.674510	0.670588	0.678431	0.686275	0.643137	0.733333	0.811765	0.823529	0.815686	0.807843
0.007843	0.133333	0.423529	0.454902	0.447059	0.466667	0.513725	0.545098	0.545098	0.568627
0.478431	0.603922	0.635294	0.666667	0.701961	0.772549	0.784314	0.764706	0.792157	0.780392
0.537255	0.560784	0.552941	0.545098	0.576471	0.596078	0.607843	0.596078	0.607843	0.623529
0.584314	0.615686	0.615686	0.596078	0.607843	0.596078	0.603922	0.639216	0.584314	0.568627

TABLE II: Evaluation Metrics

Evaluation Metrics	Formula
Recall	$\frac{TruePositive(TP)}{TruePositive(TP)+FalseNegative(FN)}$
Precision	$\frac{TruePositive(TP)}{TruePositive(TP)+FalsePositive(FP)}$
F1-score	$2 \times \frac{Precision \times Recall}{Precision+Recall}$
Accuracy	$\frac{TruePositive(TP)+TrueNegative(TN)}{Total\ number\ of\ predictions}$

TABLE III: Variation of k with p

Parameters	Value
learning_rate	0.01
comms_round	100
Input shape	(784,)
Number of classes	7
Bs (batch size)	32
num_clients	10
loss	categorical_crossentropy
metrics	accuracy
momentum	0.9

is the harmonic mean of precision and recall.

B. Results

We discuss the results in two parts, before and after the flipping of the labels.

1) *Results before flipping of the labels:* The parameters taken into consideration for building the FL model are shown in Table III while Fig. IV shows the evaluation metrics for the model.

Fig. IV shows the classification report for a multiclass classification problem, where the model is trying to predict one of the 7 different classes (0-6). The report provides precision, recall, f1 score, and support for each class. High precision implies that the model mostly predicts the correct class while a high recall means that the model can identify most of the positive instances. As the f1-score is a weighted harmonic mean of precision and recall, it balances precision and recall

TABLE IV: Classification report of the global model in FL setup before the flipping of the labels

	precision	recall	f1-score	support
0	0.00	0.00	0.00	61
1	0.33	0.01	0.02	96
2	0.30	0.08	0.13	228
3	0.00	0.00	0.00	37
4	0.69	0.99	0.81	1327
5	0.00	0.00	0.00	32
6	0.57	0.07	0.13	222
macro avg	0.27	0.16	0.16	2003
weighted avg	0.57	0.67	0.57	2003
accuracy			0.67	2003

TABLE V: Classification report for the centralized configuration

	precision	recall	f1-score	support
0	0.00	0.00	0.00	61
1	0.20	0.01	0.02	96
2	0.32	0.06	0.10	228
3	0.00	0.00	0.00	37
4	0.68	0.99	0.81	1327
5	0.00	0.00	0.00	32
6	0.53	0.08	0.14	222
macro avg	0.25	0.16	0.15	2003
weighted avg	0.56	0.67	0.56	2003
accuracy			0.67	2003

and is thus particularly useful when the classes are imbalanced. Support is the number of instances that belong to each class. The overall accuracy of the model is 67.099%. However, the accuracy can be misleading, especially when the classes are imbalanced. It's important to look at the performance of each class separately. The model correctly identifies class 4 with a high precision of 0.69 and a recall of 0.99, which is quite good. The f1-score is 0.81 for class 4. However, the model is not performing well on the 5th as well as the 0th class as the precision, recall, and f1-score are all zero. This is due to the small number of instances in those classes, which makes it difficult for the model to learn to predict them correctly. This same model was also tested on a SGD optimizer without using FL. To ensure a level playing ground, each of the hyperparameters was retained during the FL training, with the exception of the batch size. Instead of 32, the batch size in this instance was set to 320. With this configuration, the SGD will see the same number of training samples in each iteration as the global model *AI* did for each communication round in FL with this setup. Fig. V shows the detailed report for the centralized setup.

The accuracy for the centralized ML is 67.099% while the global loss is 1.55 (Fig. IV). In this configuration, the 4th class has a recall of 0.99 and a f1-score of 0.81. The precision is 0.68. The model does not perform well on the 0th class as well as the 5th class due to a smaller number of samples for both of these classes.

2) *Results after flipping of labels:* The same model was run again after a certain percentage of labels had been randomly altered. 2% of the labels were changed in the beginning, and this process continued until 20% of the labels were changed for the malicious client. The accuracy, precision, recall, and f1 scores were recorded after changing the labels from 2% to 20%. Table VI shows that the classification report changes when a certain percentage of labels are flipped. For example,

TABLE VI: Classification report of the global model in FL setup after flipping 14% of labels

	precision	recall	f1-score	support
0	0.00	0.00	0.00	61
1	0.00	0.00	0.00	96
2	0.00	0.00	0.00	228
3	0.00	0.00	0.00	37
4	0.66	0.99	0.80	1327
5	0.00	0.00	0.00	32
6	0.75	0.03	0.05	222
macro avg	0.20	0.15	0.12	2003
weighted avg	0.52	0.66	0.53	2003
accuracy			0.66	2003

TABLE VII: Change in accuracy

Percentage of labels flipped	Global accuracy	Global accuracy after label flipping	Centralized setup accuracy	Centralized setup accuracy after label flipping
2%	67.099	67.049	67.499	67.399
4%	67.099	67.099	67.499	67.149
6%	67.099	66.600	67.499	67.049
8%	67.099	66.600	67.499	67.000
10%	67.099	66.350	67.499	66.800
12%	67.099	66.151	67.499	66.400
14%	67.099	66.101	67.499	66.400
16%	67.099	66.051	67.499	66.301
18%	67.099	66.900	67.499	67.149
20%	67.099	67.249	67.499	67.299

when 14% labels are changed, there is a decrease in accuracy from 67.099% to 66.101%.

The 0th, 1st, 2nd, 3rd, and 5th classes had a precision, recall, and f1-score of 0.00 while the 4th class had a precision of 0.66, a recall of 0.99 and a f1-score of 0.80. The 6th class had a precision of 0.75, a recall of 0.03, and a f1-score of 0.05. Table VII shows the changes in accuracy before the flipping of the labels and after the flipping of the labels. The table reveals that for most cases there is a drop in accuracy when a malicious client randomly flips the label.

V. CONCLUSION

In this paper, we built a privacy-preserving federated learning model and showed the vulnerability of this model by attacking it through a malicious client. We demonstrated that this malicious client changed a certain number of samples which led to a decrease in the accuracy of the global model. We observed that for most of the cases, there is a decrease in the performance as well as the accuracy of the model. We also compared the results to a Stochastic gradient descent optimizer in a centralized learning setup. Moreover, we also compared the results before and after changing the labels and found a decrease in the performance and the accuracy of the model. In the future, rather than randomly flipping the label, optimization methods to maximally affect the accuracy could be analyzed.

REFERENCES

[1] A. Alanazi, "Using machine learning for healthcare challenges and opportunities," *Informatics in Medicine Unlocked*, vol. 30, p. 100924, 2022.

[2] A. Qayyum, J. Qadir, M. Bilal, and A. Al-Fuqaha, "Secure and robust machine learning for healthcare: A survey," *IEEE Reviews in Biomedical Engineering*, vol. 14, pp. 156–180, 2020.

[3] B. McMahan, E. Moore, D. Ramage, S. Hampson, and B. A. y Arcas, "Communication-efficient learning of deep networks from decentralized data," in *Artificial intelligence and statistics*, pp. 1273–1282, PMLR, 2017.

[4] R. A. Mehr and A. Ameri, "Skin cancer detection based on deep learning," *Journal of Biomedical Physics & Engineering*, vol. 12, no. 6, p. 559, 2022.

[5] C. Dwork, A. Roth, et al., "The algorithmic foundations of differential privacy," *Foundations and Trends® in Theoretical Computer Science*, vol. 9, no. 3–4, pp. 211–407, 2014.

[6] S. Barocas and A. D. Selbst, "Big data's disparate impact," *California law review*, pp. 671–732, 2016.

[7] "General Data Protection Regulation." <https://shorturl.at/EMPRX>.

[8] R. Shokri, M. Stronati, C. Song, and V. Shmatikov, "Membership inference attacks against machine learning models," in *2017 IEEE symposium on security and privacy (SP)*, pp. 3–18, IEEE, 2017.

[9] H. Hu, Z. Salicic, L. Sun, G. Dobbie, P. S. Yu, and X. Zhang, "Membership inference attacks on machine learning: A survey," *ACM Computing Surveys (CSUR)*, vol. 54, no. 11s, pp. 1–37, 2022.

[10] K. Chaudhuri, C. Monteleoni, and A. D. Sarwate, "Differentially private empirical risk minimization," *Journal of Machine Learning Research*, vol. 12, no. 3, 2011.

[11] E. U. Soykan, L. Karayaçay, F. Karakoç, and E. Tomur, "A survey and guideline on privacy enhancing technologies for collaborative machine learning," *IEEE Access*, vol. 10, pp. 97495–97519, 2022.

[12] C. Dwork, F. McSherry, K. Nissim, and A. Smith, "Calibrating noise to sensitivity in private data analysis," in *Theory of Cryptography: Third Theory of Cryptography Conference, TCC 2006, New York, NY, USA, March 4-7, 2006. Proceedings 3*, pp. 265–284, Springer, 2006.

[13] A. C. Yao, "Protocols for secure computations," in *23rd annual symposium on foundations of computer science (sfcs 1982)*, pp. 160–164, IEEE, 1982.

[14] N. Gessert, M. Nielsen, M. Shaikh, R. Werner, and A. Schlaefel, "Skin lesion classification using ensembles of multi-resolution efficientnets with meta data," *MethodsX*, vol. 7, p. 100864, 2020.

[15] P. Yao, S. Shen, M. Xu, P. Liu, F. Zhang, J. Xing, P. Shao, B. Kaffenberger, and R. X. Xu, "Single model deep learning on imbalanced small datasets for skin lesion classification," *IEEE transactions on medical imaging*, vol. 41, no. 5, pp. 1242–1254, 2021.

[16] J. Zhang, Y. Xie, Y. Xia, and C. Shen, "Attention residual learning for skin lesion classification," *IEEE transactions on medical imaging*, vol. 38, no. 9, pp. 2092–2103, 2019.

[17] H. Wang, Q. Qi, W. Sun, X. Li, B. Dong, and C. Yao, "Classification of skin lesions with generative adversarial networks and improved mobilenetv2," *International Journal of Imaging Systems and Technology*, 2023.

[18] A. Mahbod, G. Schaefer, C. Wang, R. Ecker, and I. Ellinge, "Skin lesion classification using hybrid deep neural networks," in *ICASSP 2019-2019 IEEE International Conference on Acoustics, Speech and Signal Processing (ICASSP)*, pp. 1229–1233, IEEE, 2019.

[19] V. Tolpegin, S. Truex, M. E. Gursoy, and L. Liu, "Data poisoning attacks against federated learning systems," in *Computer Security—ESORICS 2020: 25th European Symposium on Research in Computer Security, ESORICS 2020, Guildford, UK, September 14–18, 2020, Proceedings, Part I 25*, pp. 480–501, Springer, 2020.

[20] M. Abadi, A. Agarwal, P. Barham, E. Brevdo, Z. Chen, C. Citro, G. S. Corrado, A. Davis, J. Dean, M. Devin, S. Ghemawat, I. Goodfellow, A. Harp, G. Irving, M. Isard, Y. Jia, R. Jozefowicz, L. Kaiser, M. Kudlur, J. Levenberg, D. Mané, R. Monga, S. Moore, D. Murray, C. Olah, M. Schuster, J. Shlens, B. Steiner, I. Sutskever, K. Talwar, P. Tucker, V. Vanhoucke, V. Vasudevan, F. Viégas, O. Vinyals, P. Warden, M. Wattemberg, M. Wicke, Y. Yu, and X. Zheng, "TensorFlow: Large-scale machine learning on heterogeneous systems," 2015. Software available from tensorflow.org.

[21] P. Tschandl, C. Rosendahl, and H. Kittler, "The ham10000 dataset, a large collection of multi-source dermatoscopic images of common pigmented skin lesions," *Scientific data*, vol. 5, no. 1, pp. 1–9, 2018.